SLAC-PUB-10782

BaBar Experiment Status and Recent Results

Guglielmo De Nardo, representing the BaBar Collaboration

Naples University and INFN, Naples,
Dipartimento di Scienze Fisiche
Complesso Universitario di Monte Sant'Angelo,
via Cintia I-80126 Napoli, Italy

Abstract. The BaBar detector at SLAC PEP-II asymmetric B-Factory has collected between 1999 and 2002 a data sample of 88 millions $\Upsilon(4S) \to B\bar{B}$ decays. We present here recent measurements of branching fractions and time-dependent CP-violating asymmetries of neutral B mesons decays to several CP eigenstates. We present the results on the decays to $(c\bar{c})$ K^0_S / K^0_L, which are related in the Standard Model to the angle β of the Unitarity Triangle of the Cabibbo-Kobayashi-Maskawa quark mixing matrix. Moreover we present the branching fractions and the CP-asymmetries of charmless two body decays related to the angle α.

1 Introduction

The source of CP symmetry violation within the Standard Model of electroweak interactions is provided in an elegant way by one non-negligible complex phase in the three generation Cabibbo-Kobayashi-Maskawa quark mixing matrix (CKM) [1]. In a convenient parameterization of the matrix due to Wolfenstein [2], the phase is placed in the V_{td} and V_{ub} elements. The unitarity of the CKM matrix, among the various relations between its rows and columns, implies in particular that $V_{td}V^*_{tb} + V_{cd}V^*_{cb} + V_{ud}V^*_{ub} = 0$, which can be visualized as the closure relation of a triangle in the complex plane. This triangle is called Unitarity Triangle(U.T.). The CP symmetry is violated if that triangle has non-zero area or, which is the same, its angles, called in the literature (α, β and γ), are different from zero or π.

The measurement of CP-violating time dependent asymmetries in neutral B meson decays to CP eigenstates with charm provides a theoretically clean determination of sin 2β [3], where $\beta = arg(-V_{cd}V^*_{cb}/V_{td}V^*_{tb})$, i.e. one of the angles of the Unitarity Triangle. Asymmetry in the $B^0 \to \pi\pi$ decay, instead, allows, although in a less direct way, the extraction of sin 2α, where $\alpha = arg(-V^*_{tb}V_{td}/V^*_{ub}V_{ud})$. The ratios of the branching fractions and the CP asymmetries for $\pi\pi$ and $K\pi$ modes are sensitive to $\gamma = \pi - \alpha - \beta$, if the CKM picture of CP violation is correct.

2 The BaBar Detector

The BaBar detector has been built and is operated by a large international team of scientists and engineers. It is taking data at the SLAC PEP-II B Factory,

Work supported in part by the Department of Energy, contract DE-AC02-76SF00515
Stanford Linear Accelerator Center, Stanford University, Stanford, CA 94309

Presented at the International School on Heavy Quark Physics, 27 May - 5 Jun 2002, Dubna, Russia

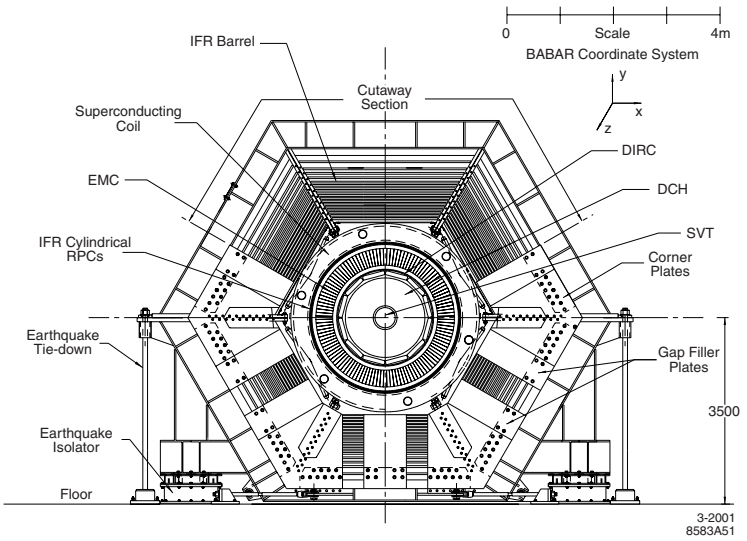

Fig. 1. BaBar detector longitudinal section.

which is an asymmetric e^+e^- collider designed to operate at a luminosity of $3 \times 10^{33}\text{cm}^{-2}\text{s}^{-1}$, at a center of mass energy of 10.58 GeV, the mass of the $\Upsilon(4S)$. The resonance decays exclusively in $B^0\bar{B}^0$ and B^+B^- pairs, providing a clean environment for B physics studies. The results reported in this paper are based on the data set collected between 1999 and June 2002, corresponding to 88 millions $\Upsilon(4S) \to B\bar{B}$ decays.

The electron beam of 9.0 GeV collides on with a positron beam of 3.1 GeV; because of the different beam energies, the center of mass frame moves in the laboratory frame with a Lorentz boost of $\beta\gamma = 0.56$. The boost makes it possible to reconstruct the decay vertices of the two B mesons, in order to measure the relative decay times and, consequently, the time dependent asymmetries.

The very small branching fractions of B mesons to CP eigenstates, the need of full reconstruction of final states, including charged and neutral particles, and the need of the measurement of the flavor of the companion B meson (B tagging), put stringent requirements in term of efficiencies and resolutions of the detector subsystems.

The detector, shown in figure 1, is divided in five subsytems: a vertex detector (SVT), a central drift chamber (DCH), a Cherenkov detector (DIRC), an electromagnetic calorimeter (EMC) and the muon and neutral hadron subsystem (IFR). A detailed description of the BaBar detector and PEP-II can be found in references [4] and [5].

3 Time Dependent CP Asymmetries

The positrons and electrons beams of PEP-II collides on with a total energy equal to the mass of the $\Upsilon(4S)$. Therefore the B mesons at PEP-II are produced in pairs via the decay $\Upsilon(4S) \to B\bar{B}$. Since the $\Upsilon(4S)$ is a spin 1 particle and the B meson has spin 0, the $B\bar{B}$ pair is produced in a p-wave. Bose statistics, thus, enforces that they oscillate coherently: if the flavor of one B is measured at any time t, the flavor of the companion B meson must be the opposite, at the same instant of time.

This nice circumstance is exploited in the measurement of time dependent CP asymmetries in the B meson decays. More precisely the experimental technique proceeds as follows [6]:

- The final state of interest is fully reconstructed. All the kinematics constraints are taken into account to select an high purity sample of events containing this decay (i.e. a sample as much free of background as possible).
- In order to measure the flavor of the reconstructed B meson(B_{CP}), the flavor of the recoiling B meson (B_{tag}) is determined, examining signatures of flavor in the rest of the event. The Bose statistics argument given above guarantees that, at the same time t_{tag} at which the B_{tag} decayed, the B_{CP} meson had the opposite flavor.
- Being interested in the time evolution of the B_{CP} decay rate, the time difference $\Delta t = t_{CP} - t_{tag}$ has to be measured. This is accomplished by measuring the distance between the vertices of the two decays. The z_{CP} measurement is provided by means of a fit to a common vertex of the charged tracks in the CP final state, which takes into account all useful topological and kinematic constraints as well (intermediate state masses, decay vertices, non-negligible flight length of long-lived particles). The remaining charged particles in the event are used as input for a dedicated vertexing algorithm to provide the other needed position measurement z_{tag}. Of course, the latter measurement, being less constrained, dominates the uncertainty on the measurement of the distance between these two vertices. Relativistic kinematics connects this position measurements to a time measurement (to a very good approximation $\Delta t = \Delta z/\gamma\beta c$).

The decay rate distributions $f_+(\Delta t)$ ($f_-(\Delta t)$) of B decays to a CP eigenstate f, when the companion B is a B^0 ($\bar{B}^0$), are given by [7]

$$f_\pm(\Delta t) = \frac{e^{-|\Delta t|/\tau_{B^0}}}{4\tau_{B^0}} \left(1 \pm S_f \sin \Delta m_d \Delta t \mp C_f \cos \Delta m_d \Delta t\right), \tag{1}$$

where $\Delta t = t_{CP} - t_{tag}$ is the difference between the proper decay times of the $B \to f$ (B_{CP}) and the companion B meson (B_{tag}), τ_{B^0} is the B^0 lifetime and Δm_d is the B^0-$\bar{B}^0$ oscillation frequency.

The S_f and C_f coefficients in equation 1 are defined in terms of a complex parameter λ_f:

$$S_f = 2\frac{\mathrm{Im}\lambda_f}{1 + |\lambda_f|^2}, \tag{2a}$$

$$C_f = \frac{1-|\lambda_f|^2}{1+|\lambda_f|^2}, \tag{2b}$$

and they vanish if CP is conserved.

If the imaginary part of λ_f, and thus S_f, is different from zero, there is CP violation in the interference between mixing and decay; if the absolute value of λ_f is different from unity, and thus C_f is non-zero, there is CP violation in decay, or direct CP violation. While the first type of CP violation has been already estabilished in the B meson system by the BABAR [8] and BELLE [9] collaborations, direct CP violation has not yet been observed only outside the neutral kaons system [10] [11].

The Standard Model predictions of CP violation can be tested determining the CP violation parameters C_f and S_f for various final states f, by means of the difference between B^0 and $\bar{B}^0$ tagged decay rates in the same CP final state f, as a function of the time difference Δt:

$$\mathcal{A}_{CP}(\Delta t) = \frac{f_+(\Delta t) - f_-(\Delta t)}{f_+(\Delta t) + f_-(\Delta t)}. \tag{3}$$

3.1 Selection of the CP sample

The first step in the measurement of the time dependent asymmetry in equation 3 is the selection of the events containing the decay mode $B \to f$ regardless of the flavor of the parent B. This is accomplished by fully reconstructing all the particles present in the decay chain (after a preselection of multi-hadron events and basic cuts on event shape in order to suppress the background from non $B\bar{B}$ events). Since the final state f is completely reconstructed, all the available kinematic constraints (invariant masses of the intermediate non stable particles), topological constraints (vertexing of the charged tracks) and particle identification information (at various level of efficiency/purity optimized to the specific mode reconstructed) are used. This allows an accurate estimate of the B meson candidate four momentum. Moreover, since the B meson is produced in the process $e^+e^- \to \Upsilon(4S) \to B\bar{B}$, the selection can take advantage of the two body kinematics of the $\Upsilon(4S)$ decay and from the fact that the beam energy is well measured. Therefore, the analyses in BaBar which perform a full reconstruction of the B use the following two kinematic variables:

$$m_{ES} = \sqrt{\left(\frac{s/2 + \boldsymbol{p}_i \cdot \boldsymbol{p}_B}{E_i}\right)^2 - \boldsymbol{p}_B^2}, \tag{4a}$$

$$\Delta E = \sqrt{s}/2 - E_B, \tag{4b}$$

where $\sqrt{s}$ is the center of mass energy, $(E_B, \boldsymbol{p}_B)$ is the B reconstructed four momentum and $(E_i, \boldsymbol{p}_i)$ is the initial state four momentum in the laboratory frame. The beam energy substituted mass variable m_{ES} is the invariant mass of the B candidate evaluated from the known initial state total energy, to determine the energy of the B candidate, and from the total momentum of the B candidate

decay products to determine the momentum. Since in this definition only the beam energy and the momenta of the particles appear, the m_{ES} variable does not depend on the mass hypotheses of the particles from which the B meson is reconstructed. Signal yields and sample purities are extracted from fits to the m_{ES} distributions of B candidates. Signal events follows a Gaussian distribution peaked at the B meson nominal mass, with a resolution dependent from the decay products. Combinatorial background, which arises from random combination of charged tracks and neutral showers from both the B mesons in $B\bar{B}$ events or from continuum events, follows an ARGUS distribution [12], whose shape has the following functional form:

$$\mathcal{A}(m_{ES}; m_0, \xi) = A_B m_{ES} \sqrt{1 - x_{ES}^2} e^{\xi(1-x_{ES}^2)}, \tag{5}$$

where $x_{ES} = m_{ES}/m_0$, where m_0 represents a kinematic limit fixed by the beam energy at 5.291 GeV/c^2, and ξ and A_B are free parameters.

The ΔE distribution is the difference between the energy of the reconstructed B candidate and the energy of the B expected from the beam, and it is distributed following a Gaussian distribution for signal events, peaked at zero if all the mass hypotheses of the B meson candidate decay products are correct.

Signal region and background sidebands are delimited in the plane defined by this two uncorrelated variables, in order to select the CP sample and to study its backgrounds. Moreover, the same technique is used to select samples of events containing charged and neutral B decays, which have been completely reconstructed, in order to measure vertexing resolutions, tagging performances or to perform branching ratios measurements.

3.2 B Flavor Tagging and Δt Resolution

Several signatures of flavor can be found examining the decay products of the recoiling B meson. The most powerful is the charge of the primary leptons from the B semileptonic decays. Indeed, in the $b \to cl\nu$ transition of the b quark (charge -1/3) to the c quark (charge +2/3) proceeds by the emission of an intermediate virtual W^-, which decays to a negative lepton and an anti-neutrino. The charge of the lepton is the same of the charge of the b quark inside the B meson, tagging the B meson flavor. Similarly, charm decays determine flavor, as well: the charge of the best identified kaon, coming from a secondary decay $b \to c \to s$ is correlated to the B flavor; or, evidence of charm in the event can be found detecting the soft pion produced in the $D^{\star+}$ decay $D^{\star+} \to D^0 \pi^+_{soft}$; in this case the pion charge is correlated to the B meson flavor.

In the BaBar experiment, multivariate tagging algorithms are defined to identify the flavor of the tagged B [6]. A neural network combines all the information from these physics based tagging algorithms in order to exploit all the correlations between the different sources of tagging information.

If the tagging algorithm incorrectly determines the flavor with a probability w, the amplitudes of the observed $B^0\bar{B}^0$ oscillations and CP asymmetries are reduced by a dilution factor $\mathcal{D} = 1 - 2w$.

Table 1. Efficiencies ϵ_i, average mistag fraction w_i, mistag fraction differences $\Delta w_i = w_i(B^0) - w_i(\bar{B}^0)$, measured for each tagging category form the combined B_{flav} and B_{CP} samples, in $\sin 2\beta$ analysis.

Cetegory	ϵ (%)	w (%)	Δw(%)	Q (%)
Lepton	9.1 ± 0.2	3.3 ± 0.6	-1.5 ± 1.1	7.9 ± 0.3
Kaon-I	16.7 ± 0.2	10.0 ± 0.7	-1.3 ± 1.1	10.7 ± 0.4
Kaon-II	19.8 ± 0.3	20.9 ± 0.8	-4.4 ± 1.2	6.7 ± 0.4
Inclusive	20.0 ± 0.3	31.5 ± 0.9	-2.4 ± 1.3	2.7 ± 0.3
Total	65.6 ± 0.5			28.1 ± 0.7

On the basis of the output of the physics-oriented algorithms and the estimated mistag probability, each event is assigned to one of four hierarchical and mutually exclusive categories. The Lepton category contains events with a well identified lepton and a supporting kaon tag, if present. Events with a kaon tag and a soft pion with opposite charge and consistent flight direction are assigned to the Kaon-I category. Events with a kaon without a soft pion are assigned to the Kaon-I or to the Kaon-II category on the basis of the estimated mistag probability. The rest of the events are excluded or assigned to the Inclusive category depending on the estimated mistag probability. The quality of the tag depends on both its efficiency ϵ (how many times the algorithm is able to give an answer) and its mistag probability (how many times the output is wrong). The quantitative figure of merit is the effective tagging efficiency $Q = \sum_i \epsilon_i (1 - 2w_i)^2$, since the contribution to the statistical uncertainty in the asymmetry measurement is $\sigma_{asym} = \sigma_0/\sqrt{NQ}$. The performances of the tagging algorithms in the $\sin 2\beta$ analysis are summarized in table 1.

Another important effect that must be taken into account is the finite resolution of the detector in the measurement of the time difference Δt. The time evolution of the rates of tagged events $f_{\pm}(\Delta t)$ must be convolved with a resolution function $\mathcal{R}(\delta t = \Delta t - \Delta t_{true}; \boldsymbol{a})$, where Δt and Δt_{true} are the measured and true time difference between the tagging B decay and reconstructed B decay and $\boldsymbol{a}$ are the parameters of the resolution function.

In order to measure the w_i mistag rates and the a_i parameters of the Δt resolution functions, a data sample of events with a neutral B meson fully reconstructed in $B^0 \to D^{(*)-}\pi^+/\rho^+/a_1^+$ or $B^0 \to J/\psi K^{*0}(K^{*0} \to K^+\pi^-)$, and the corresponding flavor conjugates modes, has been used (B_{flav}). In these decays, the flavor of the reconstructed B meson is correlated to the sign of the D meson or the kaon in the final state. Therefore, the dilutions due to mistagging can be extracted studying the time dependent rate of the $B^0\bar{B}^0$ oscillations on these data sample.

The mistag rates w_i and the Δt resolution parameters $\boldsymbol{a_i}$, for each tagging category i, can be extracted performing an unbinned maximum likelihood fit to the time distribution of the fully reconstructed B_{flav} sample:

$$\ln \mathcal{L}_{mix} = \sum_{i}^{tagging} \left[\sum_{unmixed} \ln h_+(\Delta t; w_i, \boldsymbol{a}_i) + \sum_{mixed} \ln h_-(\Delta t; w_i, \boldsymbol{a}_i) \right] \otimes \mathcal{R}(\delta t, \boldsymbol{a}), \tag{6a}$$

$$h_\pm = \frac{e^{-|\Delta t|/\tau_B^0}}{4\tau_{B^0}} \left[1 \pm (1-2w)\cos \Delta m_d \Delta t\right], \tag{6b}$$

where the sum is over the taging category i, mixed (unmixed) is for events in which the B mesons pair is found to have opposite (same) flavor, and the $h_\mp$ are the probability to find the pair in opposite (same) flavor, as a function of the decay time difference, according to the known phenomenon of flavor oscillations.

In the limit of no dependence from the reconstructed side, the same mistag rate parameters w_i and resolution parameters a_i can be used for the CP asymmetry measurement, and the functions $f_\pm$ in equation 3, describing the decay rates have to be substituted by the following function which take into account the experimental effects ($f_\pm \rightarrow \mathcal{F}_\pm$):

$$\mathcal{A}_{CP}(\Delta t) = \frac{\mathcal{F}_+(\Delta t) - \mathcal{F}_-(\Delta t)}{\mathcal{F}_+(\Delta t) + \mathcal{F}_-(\Delta t)}, \tag{7a}$$

$$\mathcal{F}_\pm(\Delta t; w, \boldsymbol{a}) = \frac{e^{-|\Delta t|/\tau_{B^0}}}{4\tau_{B^0}} \left[1 \pm \mathcal{D}\left(\frac{2\mathrm{Im}\lambda}{1+|\lambda|^2}\sin \Delta m_d \Delta t - \frac{1-|\lambda|^2}{1+|\lambda|^2}\cos \Delta m_d \Delta t\right)\right] \tag{7b}$$

The value of the free parameter λ can be extracted using the B_{CP} sample with the tagging and vertexing requirements by maximizing the likelihood:

$$\ln \mathcal{L}_{CP} = \sum_{i}^{tagging} \left[\sum_{B^0 tagged} \ln \mathcal{F}_+(\Delta t; w_i, \boldsymbol{a}_i, \lambda) + \sum_{\bar{B}^0 tagged} \ln \mathcal{F}_-(\Delta t; w_i, \boldsymbol{a}_i, \lambda) \right] \otimes \mathcal{R}(\delta t, \boldsymbol{a}) \tag{8}$$

where B^0 tagged and $\bar{B}^0$ tagged is for events identified by the tagging algorithm as containing a recoiling B^0 or $\bar{B}^0$. In practice, the fit is performed simultaneously on the combined B_{flav} and B_{CP} sample with a likelihood constructed with the sum of the likelihoods in equations 6a and equation 8, to determine the CP violating parameter, the mistag fractions, the vertex resolution parameters, including additional terms to account for backgrounds and their time dependence.

4 Measurement of the CP-violating Asymmetry Amplitude sin 2β

In the Standard Model the most abundant decays of neutral B meson, sensitive to the value of the β angle of the Unitarity Triangle, are due to the quark

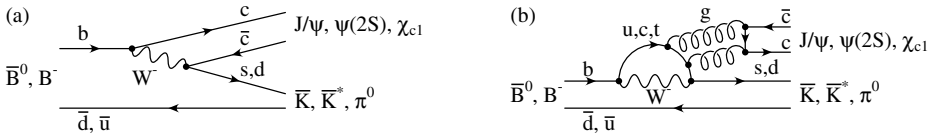

Fig. 2. (a) Tree level (a) and penguin (b) amplitudes for $b \to c\bar{c}s(d)$ transition and corresponding particles in the final state. (b) Penguin amplitude for

level process $b \to c\bar{c}s$, whose Feynman diagrams are shown in figure 2. The corresponding final states are a $c\bar{c}$ resonance ($J/\psi, \psi(2S), \chi_c, \eta_c, etc.$) and a K^0 or a K^{*0}.

The penguin amplitude, which, in principle, contributes to these decays, actually does not modify the value of the parameter λ, since it shares the same weak phase with the leading tree amplitude. Therefore, λ can be written in terms of CKM matrix elements as:

$$\lambda_f = \eta_f^{CP} \times \left(\frac{V_{tb}^* V_{td}}{V_{tb} V_{td}^*}\right) \times \left(\frac{V_{cs}^* V_{cb}}{V_{cs} V_{cb}^*}\right) \times \left(\frac{V_{cd}^* V_{cs}}{V_{cd} V_{cs}^*}\right), \tag{9}$$

where the three CKM factors are due to CP violation in the $B^0\bar{B}^0$ mixing, which is dominated by the top quark loop, to CP violation in the $b \to c\bar{c}s$ and $\bar{b} \to c\bar{c}\bar{s}$ amplitudes, and to the amplitude of $K^0 - \bar{K}^0$ mixing.

Using unitarity relations and the definition of the β angle, the expression simplifies to:

$$\lambda_f = \eta_f^{CP} e^{-2i\beta}, \tag{10}$$

where η_f^{CP} is the CP eigenvalue of the final state f, equal to -1 if the neutral kaon is a K_S^0, or equal to +1 if the neutral kaon is a K_L^0; the final state in K^{*0} is not a pure CP eigenstate, and requires an angular analysis, to separate the CP even and CP odd components and extract the CP violation parameter λ.

Since λ is a pure phase, the CP violating parameters of equations 2a and 2b, and the time dependent CP asymmetry of equation 3 become:

$$\begin{aligned} C_f &= 0 \\ S_f &= -\eta_f^{CP} \sin 2\beta \\ \mathcal{A}_{CP}(\Delta t) &= -\eta_f^{CP} \sin 2\beta \sin(\Delta m_d \Delta t), \end{aligned} \tag{11}$$

In figure 3 are shown the m_{ES} distributions for the events containing a K_S^0 or a K^{*0} and the ΔE distribution for the $J/\psi K_L^0$ candidates. In the latter case, the background distribution is taken from Monte Carlo simulation for the $B^0 \to J/\psi X$ background, and from sidebands in data for the fake J/ψ background.

The measurement of $\sin 2\beta$ is performed following the method described in section 3. The value of $\sin 2\beta$ is extracted from an unbinned maximum likelihood fit. The used Likelihood function is the sum of the likelihoods in equation 6a and 8, assuming $|\lambda| = 1$, maximized simultaneously on the combined B_{CP} and B_{flav} samples:

$$\ln \mathcal{L} = \ln \mathcal{L}_{CP} + \ln \mathcal{L}_{mix}. \tag{12}$$

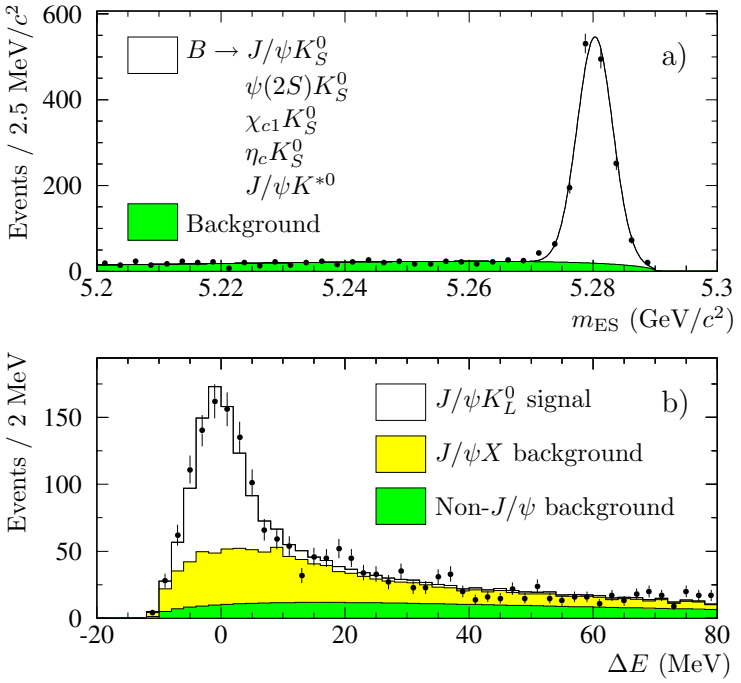

Fig. 3. Distributions for the CP sample after requiring the tagging and the vertexing: a) Energy Substituted mass m_{ES} for $J/\psi K^0_S$, $\psi(2S)K^0_S$, $\chi_{c1}K^0_S$, $\eta_c K^0_S$ $and J/\psi K^{*0}$ decay modes; b) ΔE for the $J/\psi K^0_L$ mode.

There are 34 free parameters in the fit: On the signal side the $\sin 2\beta$ parameter itself (1), the average mistag fraction w and the differences δw between mistag probability in B^0 and $\bar{B}^0$ for each tagging category (8), the parameters for the Δt resolution(8); on the background side parameters for the background time dependence (6), Δt resolution (3), and mistag fraction (8). The extracted value of $\sin 2\beta$ is [13]:

$$\sin 2\beta = 0.741 \pm 0.067(stat.) \pm 0.033(syst.). \tag{13}$$

The distributions of B^0 and $\bar{B}^0$ tagged decays as a function of Δt and the asymmetry, together with the fit result, are shown in figure 4. The dominant sources of systematic uncertainty are:

- uncertainties in the level, composition and CP asymmetry of the background (0.023);
- the assumed parameterization of the Δt resolution function (0.017) due to residual uncertainties in the vertex detector alignment;
- differences between the flavor and the CP sample mistag fraction (0.012).

The large size of the B_{CP} sample allows several consistency checks. This includes comparing the fit results by decay mode, tagging category, and B_{tag}

Table 2. Number of events N_{tag} after tagging and vertexing requirements, signal purity P and fitted value of $\sin 2\beta$ for various subsamples of the B_{CP}, B_{flav} and charged B control sample

Sample	N_{tag}	P (%)	$\sin 2\beta$
$(c\bar{c})K^0_S$	1506	94	0.76 ± 0.07
$J/\psi K^0_L$	988	55	0.72 ± 0.16
$J/\psi K^{*0}(K^* \to K^0_S\pi^0)$	147	81	0.22 ± 0.52
Full CP Sample	2641	78	0.74 ± 0.07
$(c\bar{c})K^0_S$ only			
$J/\psi K^0_S(K^0_S \to \pi^+\pi^-)$	974	97	0.82 ± 0.08
$J/\psi K^0_S(K^0_S \to \pi^0\pi^0)$	170	89	0.39 ± 0.24
$\psi(2S)K^0_S(K^0_S \to \pi^+\pi^-)$	150	97	0.69 ± 0.24
$\chi_{c1}K^0_S$	80	95	1.01 ± 0.40
$\eta_c K^0_S$	132	73	0.59 ± 0.32
Lepton	220	98	0.79 ± 0.11
Kaon I	400	93	0.78 ± 0.12
Kaon II	444	93	0.73 ± 0.17
Inclusive	442	92	0.45 ± 0.28
B^0 tags	740	94	0.76 ± 0.10
$\bar{B}^0$ tags	766	93	0.75 ± 0.10
Fully Reconstructed Sample			
B_{flav}	25375	85	0.02 ± 0.02
B^+	22160	89	0.02 ± 0.02

flavor. The results of fits to these subsamples are found to be statistically consistent. Fits to the control samples of non-CP decay modes (the B_{flav} sample and fully reconstructed charged B decays sample) indicated no statistically significative asymmetry, as expected. This breakdown of the data sample and the results of checks are reported in table 2.

The parameter $|\lambda|$ has been measured as well, repeating the fit procedure, with $|\lambda|$ allowed to float, on the $\eta_f = -1$ CP sample, for which the effect of the backgrounds is very limited. In this case, five additional parameters have been added, to account for differences in tagging and reconstruction efficiencies for B^0 and $\bar{B}^0$, which may simulate an artificial asymmetry. The result of the fit for $|\lambda|$ is:

$$|\lambda| = 0.948 \pm 0.051(stat.) \pm 0.017(syst.). \tag{14}$$

which is consistent with the hypothesis of pure phase and consequently no direct CP violation.

5 Measurement of the CP violating amplitude $\sin 2\alpha$

The time-dependent CP-violating asymmetries in the decay $B^0 \to \pi^+\pi^-$ are related to the angle α of the Unitarity Triangle. If the decay proceeds purely

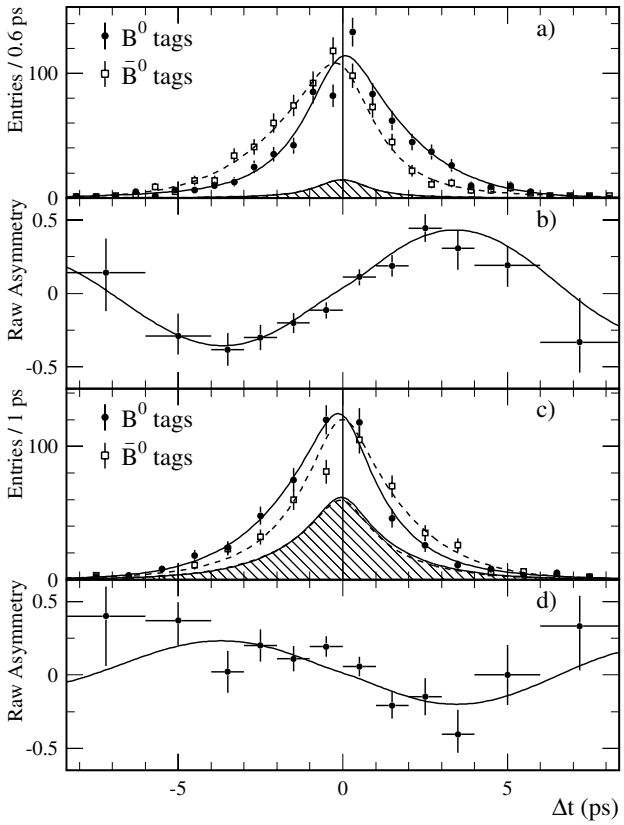

Fig. 4. a) Number of candidates for the $\eta_f = -1$ sample, in the signal region with a B^0 tag (full boxes data, solid line fit) and $\bar{B}^0$ tag (empty box data, dashed line fit). The shaded region represent the residual background. b) Raw asymmetry $(N_{B^0} - N_{\bar{B}^0})/(N_{B^0} + N_{\bar{B}^0})$, as a function of Δt. c) and d) Same content as a) and b) for the $J/\psi K^0_L$ mode ($\eta_f = +1$).

through the $b \to u$ tree amplitude, the complex parameter $\lambda_{\pi\pi}$, would be

$$\lambda(B^0 \to \pi^+\pi^-) = \left(\frac{V^*_{tb}V_{td}}{V_{tb}V^*_{td}}\right)\left(\frac{V^*_{ub}V_{ud}}{V_{ub}V^*_{ud}}\right). \tag{15}$$

Similarly to the $\sin 2\beta$ case, it would be $C_{\pi\pi} = 0$ and $S_{\pi\pi} = \sin 2\alpha$, where $\alpha = arg(-V^*_{tb}V_{td}/V^*_{ub}V_{ud})$.

Unfortunately, $b \to d$ penguins amplitudes can contribute in a significant way to the total amplitude of the process, so that they cannot be neglected. The tree and the penguin Feynman diagrams are showed in figure 5. Considering both the contributions, λ acquires a magnitude different from 1 and a shift in the phase:

$$\lambda(B^0 \to \pi^+\pi^-) = e^{-2i\alpha}\frac{1 + |P/T|\, e^{i\delta}e^{i\gamma}}{1 + |P/T|\, e^{i\delta}e^{-i\gamma}}$$

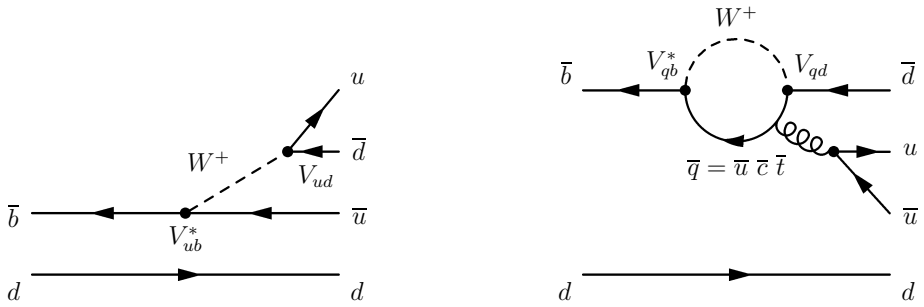

Fig. 5. Tree (left) and penguin (right) Feynman diagrams for the decay $B^0 \to \pi^+\pi^-$

$$\begin{aligned} C_{\pi\pi} &\propto \sin\delta \neq 0, \\ S_{\pi\pi} &= \sqrt{1 - C^2_{\pi\pi}} \sin 2\alpha_{eff}, \end{aligned}$$

where δ and γ are the the strong and weak phase differences between the tree amplitude T and the penguin amplitude P. Therefore, the time dependent CP-asymmetry permits the observation of α_{eff}, which depends on the magnitudes of relative strong phase δ and the relative weak phase γ between the tree and penguins amplitudes. The implication is that the relative magnitudes of the two contributions have to be determined in order to extract the value of $\sin 2\alpha$. Several approaches have been proposed to obtain information on α in the presence of penguins [14] [15] [16] [17].

Moreover, from the experimental point of view, the smallness of $|V_{ub}|$ makes small the branching fractions of these decay modes ($10^{-5} \div 10^{-6}$); the necessity to suppress an high level of combinatoric background, makes the analysis a great experimental challenge.

5.1 Sample Selection of the Charmless Decays $B^0 \to h^+h^-$

The yields and the CP parameters are extracted from an unbinned maximum likelihood fit, which is described in the next section. The probability density functions used in the Likelihood function are chosen to discriminate between $B^0 \to h^+h^-$ signal and $q\bar{q}$ background, and among the various signals ($B^0 \to \pi\pi/K\pi/KK$).

For signal decays the ΔE and m_{ES} are Gaussian distributed with a resolution of 26 MeV and 2.6 MeV, respectively. Since the B candidate energy is determined in the pion hypothesis, the ΔE is shifted towards negative values, if a kaon is present in the final state. For example, the shift of mean of the Gaussian probability density function for $K\pi$ decays is $\delta\mu_{\Delta E} = -\gamma\left(\sqrt{m_K^2 - p^2} - \sqrt{m_\pi^2 - p^2}\right)$, where p is the kaon momentum. The average value of the shift is -45 MeV for the $K\pi$ case and -91 MeV for the KK case. The parameters of the m_{ES} and ΔE distributions are fitted from a sample of $B^- \to D^0\pi^-$ and the systematic uncertainty is determined by varying the m_{ES} peak position and resolution. The

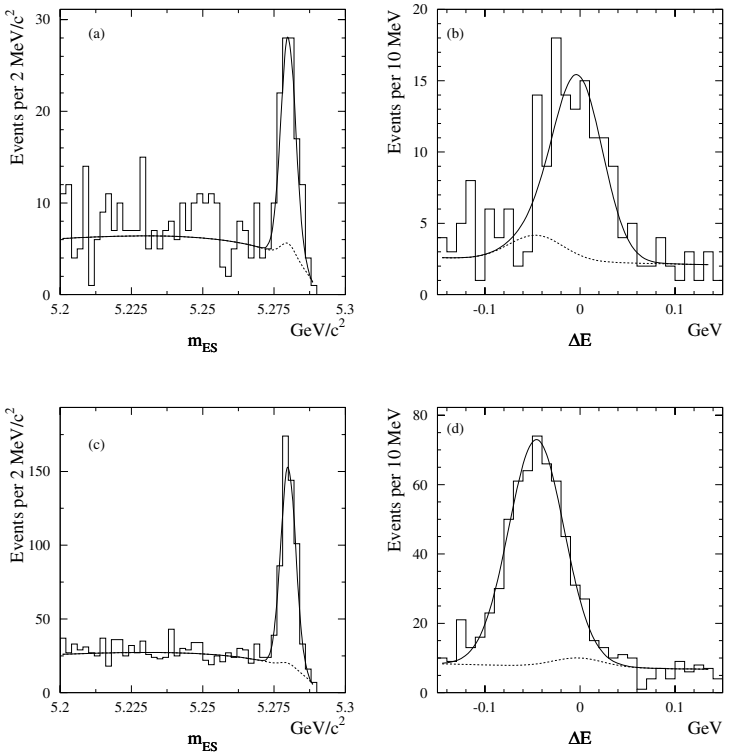

Fig. 6. Distributions of energy substituted mass m_{ES} (left) and energy difference ΔE (right) for events enhanced in signal. Top plots are $B^0 \to \pi\pi$ candidate events and bottom plots are $B^0 \to K\pi$ candidate events. Solid curve represent the projections of the maximum likelihood fit, while dashed curves represent the continuum and $\pi\pi \leftrightarrow K\pi$ cross-feed backgrounds.

m_{ES} and ΔE distributions for signal, enhanced in $B \to \pi\pi$ and $B \to K\pi$, are shown in figure 6.

Residual background from $e^+e^- \to q\bar{q}(q = u, d, s, c)$, is suppressed by event topology [18], since in $B\bar{B}$ events charged tracks and energy releases of neutral particles are more uniformly distributed over the solid angle with respect to the more jet-like continuum events.

Kinematics information from particles in the event, not used to build the B candidate, are combined in a Fisher discriminant [19]:

$$\mathcal{F} = 0.53 - 0.60 \times \sum_i p_i^* + 1.27 \times \sum_i p_i^* \left|\cos\theta_i^*\right|^2 , \tag{16}$$

where p_i^* is the momentum of the particle i in the center of mass frame and θ_i^* is the angle between the particle momentum and the B thrust axis in the center of mass frame. The value of the coefficients of the Fisher discriminant in equation

Table 3. Summary of the results for the branching fraction B and the asymmetry $\mathcal{A}$ in charmless B decays. The upper limits on B($B^0 \to K^+K^-$) and B($B^0 \to \pi^0\pi^0$) corresponds to a 90% C.L.

Mode	$B(10^{-6})$	$\mathcal{A}$	$\mathcal{A}$ 90% C.L.
$\pi^+\pi^-$	$4.6 \pm 0.6 \pm 0.2$		
$K^+\pi^-$	$17.9 \pm 0.9 \pm 0.7$	$-0.102 \pm 0.050 \pm 0.016$	[-0.188, -0.016]
K^+K^-	< 0.6		
$\pi^+\pi^0$	$5.5^{+1.0}_{-0.9} \pm 0.6$	$0.03^{+0.18}_{-0.17} \pm 0.02$	[-0.32,0.27]
$K^+\pi^0$	$12.8^{+1.2}_{-1.1} \pm 1.0$	$-0.09 \pm 0.09 \pm 0.01$	[-0.24,0.06]
$K^0\pi^0$	$10.4 \pm 1.5 \pm 0.8$	$0.03 \pm 0.36 \pm 0.09$	[-0.58,0.64]
$\pi^0\pi^0$	< 3.6		

16 are, by definition, those which maximize the separation between signal and background. The shape of $\mathcal{F}$ is determined from Monte Carlo for the signal and m_{ES} sideband for background.

Particle identification is required to discriminate between the pion and kaon hypotheses. This is accomplished using the measurements from the Cherenkov detector.

The probability density function of the difference between the measured Cherenkov angle θ_c and the expected angle in the pion and in the kaon hypothesis, normalized by the error σ_{θ_c} is added to the Likelihood function for both the two charged particles. The parameters of the function are measured from a pure data sample of $D^* \to D^0\pi^+$, $D^0 \to K^-\pi^+$ decays.

5.2 CP asymmetries and Branching Fractions Measurement of the charmless decays $B^0 \to h^+h^-$

The yields and the CP parameters are extracted from an unbinned maximum likelihood fit simultaneously on the B_{flav} and the h^+h^- sample, as usual. The sample is assumed to be composed in eight signal and background components: $\pi^+\pi^-$, $K^+\pi^-$, π^+K^-, K^+K^-. For both signal and backgrounds, $K\pi$ events are parameterized as the sum $N_{K\pi}$ and the asymmetry $\mathcal{A}_{K\pi} = (N_{K^-\pi^+} - N_{K^+\pi^-})/(N_{K^-\pi^+} + N_{K^+\pi^-})$. The probability for each event to be a given signal or background hypothesis is evaluated as the product of the probability density functions of the variables $(m_{ES}, \Delta E, \mathcal{F}, \theta_c^+, \theta_c^-, \Delta t)$.

The Likelihood for a candidate j in the tagging category k is defined to be the sum for every hypothesis i of the product of the yield N_i , the tagging efficiency $\epsilon_{i,k}$ and the probability $P_{i,k}$. The extended likelihood function for the category k is:

$$\mathcal{L}_k = exp\left(-\sum_i N_i\epsilon_{i,k}\right)\prod_j\left(\sum_i N_i\epsilon_{i,k}P_{i,k}(\boldsymbol{x}_j;\boldsymbol{\alpha}_i)\right). \qquad (17)$$

The total likelihood is the product of the likelihood for each category, and the free parameter $\boldsymbol{\alpha}$ are determined by minimizing - $\ln\mathcal{L}$.

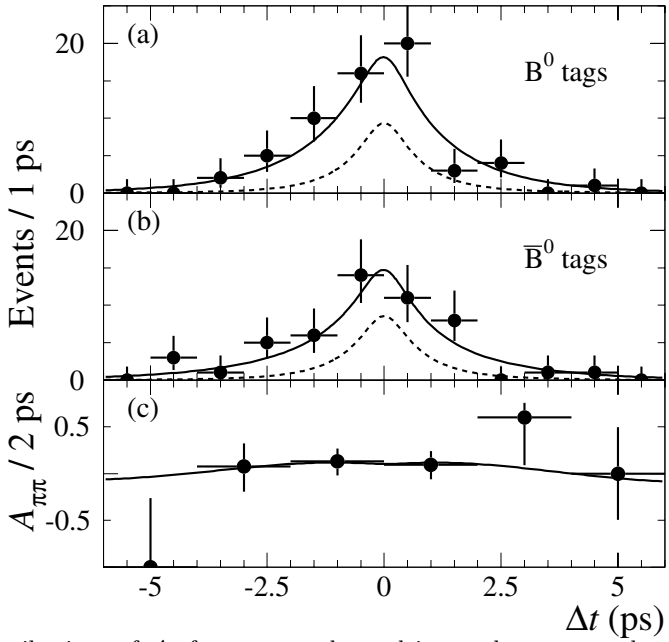

Fig. 7. Distributions of Δt for events enhanced in $\pi\pi$ decays tagged as (a) B^0, (b) $\bar{B}^0$. (c) Distribution of the asymmetry $\mathcal{A}_{\pi\pi}$ as a function of Δt. Solid curve is the projection of the maximum likelihood fit, dashed curves represent the residual $q\bar{q}$ and $K\pi$ events.

In order to minimize the systematic uncertainty, the fit for the branching fraction measurement is performed not requiring tagging and vertexing of the recoiling B, and not requiring the Δt information. In this case the number of free parameters is 16 and includes the signal and background yields (6), the $K\pi$ asymmetries (2), and the background shape parameters for $m_{ES}, \Delta E, \mathcal{F}$ (8). Table 3 shows the summary of the results from the fit.

In order to extract the CP violating parameter $S_{\pi\pi}$ and $C_{\pi\pi}$, tagging and Δt informations are added. Since an asymmetry between tagging B^0 and $\bar{B}^0$ events can result in an artificial asymmetry in the $C_{\pi\pi}$ term, the mistag probabilities and the tagging efficiencies are included separately for B^0 and $\bar{B}^0$. The combined fit to signal and flavor sample is performed with 76 free parameters:

- The CP violating parameters $S_{\pi\pi}$ and $C_{\pi\pi}$ (2).
- Signal and background yields with N_{KK} fixed to zero (5).
- $K\pi$ asymmetries (2).
- signal and background tagging efficiencies (16).
- signal and background tagging efficiencies asymmetries (16).
- signal mistag and mistag asymmetries (8).
- signal resolution functions (9).
- the background shape parameters for m_{ES} (5), ΔE (2), $\mathcal{F}$ (5) and Δt (6).

Table 4. Expected statistical and systematic uncertainties on the CP violating parameters $\sin 2\beta$ and $sin2\alpha_{eff}$ at the present moment, and after 500 fb^{-1} and 2 ab^{-1} of integrated luminosity.

Parameter	Channel	σ (stat)/ σ (syst) at 81 fb^{-1}	σ (stat)/ σ (syst) at 0.5 ab^{-1}	σ (stat)/ σ (syst) at 2.0 ab^{-1}
$\sin 2\beta$	Golden	0.07 / 0.03	0.031/ 0.016	0.018 / 0.015
$\sin 2\alpha_{eff}$	$\pi^+\pi^-$	0.34 / 0.05	0.12 / 0.03	0.06 / 0.03
$C_{\pi\pi}$	$\pi^+\pi^-$	0.25 / 0.04	0.10 / 0.03	0.05 / 0.03

The fitted decay rates and asymmetry distributions for the $B^0 \to \pi^+\pi^-$ case are shown in figure 7. The fitted values for the CP violating parameters $C_{\pi\pi}$ and $S_{\pi\pi}$ are [20]:

$$S_{\pi\pi} = 0.02 \pm 0.34(stat) \pm 0.05(syst), \tag{18a}$$

$$C_{\pi\pi} = -0.30 \pm 0.25(stat) \pm 0.04(syst). \tag{18b}$$

The systematic uncertainty on $S_{\pi\pi}$ and $C_{\pi\pi}$ are dominated by the imperfect knowledge of the probability density functions shapes and fit bias.

Since the extraction of the α angle from the $B^0 \to \pi^+\pi^-$ CP asymmetry is complicated by the presence of the penguin amplitudes, additional measurements of isospin related decays $B^+ \to \pi^+\pi^0$ and $B^0 \to \pi^0\pi^0$ may help. Moreover, the measurements of $B \to K\pi$ decays branching fractions and asymmetries, can be related to α and γ angle, by means of various models [14] [21] [22] [23], based on different theoretical assumptions. The detail of the analysis, which follows the general method described for h^+h^- modes, can be found in [24] [25] and the results are reported in table 3 for completeness.

6 Conclusions

The BaBar experiment has collected a data set of 88 millions $\Upsilon(4S)$ decays from 1999 to June 2002. The new measurement of $\sin 2\beta = 0.741 \pm 0.067 \pm 0.033$ shows that BaBar is starting to provide a precision measurement of this important parameter of the Standard Model. CP violation is now well established, and at the present moment it is fully consistent with the Standard Model expectation.

In figure 8 it is shown a comparison [26] between the BaBar $\sin 2\beta$ direct measurement and the indirect determination of an allowed region of the Unitarity Triangle apex position in the (ρ,η) plane from the measurements of $|\epsilon_K|$, $|V_{ub}/V_{cb}|$, Δm_d and Δm_s. The BaBar and Belle direct measurements differ qualitatively from the indirect constraint, because for the former the size of the region is determined by experimental uncertainties of statistical origin, while the latter is determined mainly by theoretical uncertainties of more difficult interpretation.

With the present data set, the experiment is already sensitive to more rare $\sin 2\beta$ modes, like $B^0 \to D^*D^*$ [27], $J/\psi\pi^0$ [28] or ΦK^0_S [29], which not only enrich the sample but may show up new physics, as well.

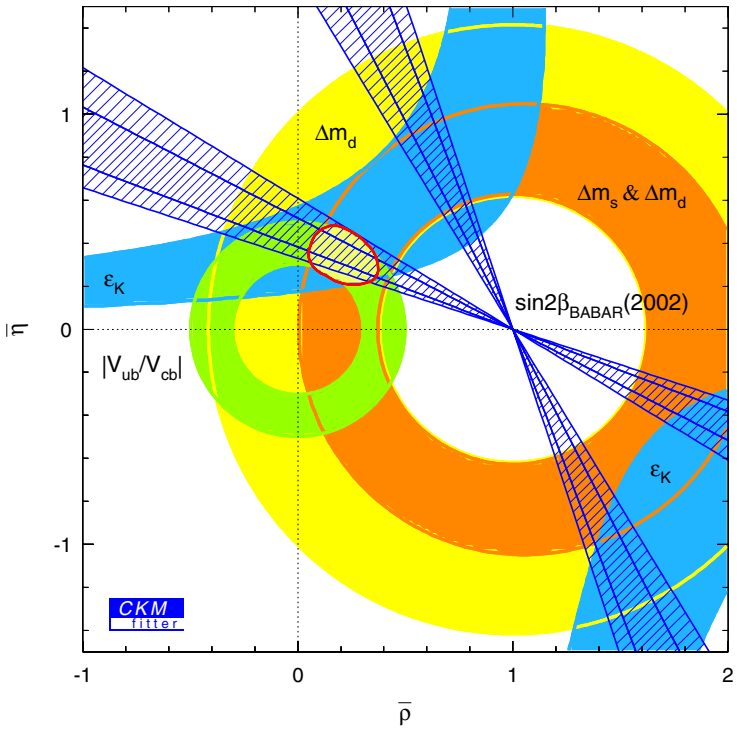

Fig. 8. Indirect constraints on the position of the Unitarity Triangle apex in the $\rho - \eta$ plane, not including the measurement of $\sin 2\beta$. The fit procedure is described in reference [26]. The BaBar measurement of $\sin 2\beta$ is represented by the two hatched regions corresponding to one and to two standard deviations.

Moreover, the $\sin 2\beta$ measurement on more abundant and clean sample of golden modes will continue to be not limited by the systematic uncertainties till 0.5 ab^{-1} of integrated luminosity has been collected. At the expected luminosity of $1.6 \times 10^{34}\text{cm}^{-2}\text{s}^{-1}$, this would happen in 2006. Before then, the measurement accuracy will continue to improve with the increasing statistics.

Measurements in the charmless B decays did not show any evidence of CP violation. Branching fraction of the various charged and neutral modes have been determined, allowing isospin analyses in order to extract, or put limits on, the parameter $\sin 2\alpha$.

Table 4 shows the uncertainties on $\sin 2\beta, \sin 2\alpha_{eff}$ and $C_{\pi\pi}$ at the present moment, and after an integrated luminosity of 0.5 ab^{-1} and 2.0 ab^{-1}, respectively.

References

1. N.Cabibbo, Phys. Rev. Lett. **10**, 531 (1963) ;
M.Kobayashi and T.Maskawa Prog. Th. Phys. **49**, 652 (1973).

2. L. Wolfenstein, Phys. Rev. Lett. **51**, 1945 (1983).
3. A.B. Carter and A.I. Sanda, Phys. Rev. D **23**, 1567 (1981); I.I. Bigi and A.I. Sanda, Nucl. Phys. B **193**, 85 (1981).
4. BABAR Collaboration, B.Aubert et al., Nucl. Instr. and Meth. A **479** (2002) 1.
5. PEP-II: an Asymmetric B Factory, Conceptual Design Report, SLAC-418, LBL-5379 (1993)
6. BABAR Collaboration, B.Aubert et al., Phys. Rev. D **66**, 032003 (2002).
7. See for example the review by L.Wolfenstein in Phys. Rev. D **66** 010001 (2002).
8. BABAR collaboration, B.Aubert et al., Phys. Rev. Lett. **87**, 091801 (2001)
9. BELLE collaboration, K.Abe et al., Phys. Rev. Lett. **87**, 091802 (2001)
10. NA48 collaboration, Phys. Lett B **544** 97-112 (2002)
11. KTeV collaboration, hep-ex/0208007, submitted to Phys. Rev. D
12. ARGUS Collaboration, H. Albrecht et al., Phys. Lett. B **241**, 278 (1990).
13. BABAR Collaboration, B. Aubert et al., Phys. Rev. Lett. **89**, 201802 (2002).
14. M.Beneke, G.Buchalla, M.Neubert and C.T. Sachrajda, Nucl. Phys. B **606**, 245 (2001);.
15. Y. Grossman and H.R. Quinn, Phys. Rev. D **59**, 054007 (1999).
16. M. Gronau, D.London, N.Sinha and R.Sinha, Phys. Lett. B **514**, 315 (2001).
17. M. Gronau and J. Rosner, Phys. Rev. D **65**, 090012 (2002).
18. G.C. Fox and S. Wolfram, Phys. Rev. Lett. **41**, 1581 (1978).
19. R.A. Fisher, Annals of Eugenics **7** 179 (1936).
20. BABAR Collaboration, B. Aubert et al., SLAC-PUB-9317, hep-ex/0207055 submitted to Phys. Rev. Lett.
21. M.Ciuchini, E. Franco, G. Martinelli, M. Pierini and L.Silvestrini, Phys. Lett. B **515**, 33 (2001).
22. Y.Y. Keum, H.N. Li and A.I. Sanda, Phys. Rev. D **63** 054008 (2001).
23. C.Isola, M.Ladisa, G. Nardulli, T.N. Pham and P. Santorelli, Phys. Rev. D **65**, 094005 (2002).
24. BABAR Collaboration, B. Aubert et al., SLAC-PUB-9304 hep-ex/0207065
25. BABAR Collaboration, B. Aubert et al., SLAC-PUB-9310 hep-ex/0207063
26. A.Hocker et al., Eur. Phys. J. C **21**, 225 (2001)
27. BABAR Collaboration, B. Aubert et al., SLAC-PUB 9299, hep-ex/0207072
28. BABAR Collaboration, B. Aubert et al., SLAC-PUB 9298, hep-ex/0207058
29. BABAR Collaboration, B. Aubert et al., SLAC-PUB 9297, hep-ex/0207070